Structural and Electronic Properties of the Heme Cofactors in a Multi-Heme Synthetic Cytochrome†

William A. Kalsbeck,‡ Dan E. Robertson,§,|| Ravindra K. Pandey,⊥,# Kevin M. Smith,⊥ P. Leslie Dutton,§ and David F. Bocian*,‡

The Departments of Chemistry, University of California, Riverside, California 92521 and University of California, Davis, California 95616, and The Johnson Research Foundation, Department of Biochemistry and Biophysics, University of Pennsylvania, Philadelphia, Pennsylvania 19104

Received November 8, 1995; Revised Manuscript Received January 22, 1996⊗

ABSTRACT: Resonance Raman, absorption, and electron paramagnetic resonance spectra are reported for a water soluble, synthetic cytochrome. The protein is a variant of the cytochrome *b* maquette described by Robertson et al. [Robertson, D. E., et al. (1995) *Nature 368*, 425−432] and is composed of 62 amino acid residues arranged in a di-α-helical unit which dimerizes in solution to form a four-helix bundle. Each di-α-helical unit contains histidine residues at the 10,10′ positions which serve as ligands to the hemes. When protoheme IX is incorporated, both hemes in the dimer are bis-ligated and low spin. The two hemes are inequivalent with respect to both binding affinity and redox properties. To investigate the properties of the heme cofactors, spectroscopic studies were conducted on peptides reconstituted with protoheme IX (PHa) and several related variants. These hemes include 2-vinyldeuteroheme (2-VDH), 4-vinyldeuteroheme (4-VDH), protoheme III (PHs), and 1-methyl-2-oxomesoheme XIII (2-OMH). Collectively, the spectroscopic studies reveal the following: (1) 2-VDH, 4-VDH, and 2-OMH bind to the protein and form bis-ligated low-spin complexes similar to PHa. The structures of the two hemes in the dimers are identical as are the immediate protein environments around the bound cofactors. These results indicate that the redox inequivalence of the two hemes is due to heme−heme electronic interactions rather than structural and/or environmental differences between the two cofactors. (2) The two hemes in the dimer are arranged in a edge-to-edge arrangement wherein the oxo group (2-OMH) or the vinyl group(s) are in the hydrophobic interface between the two units which comprise the dimer. The propionic acid tails point outward toward the hydrophilic region and extend into the solvent. (3) The PHs protein differs from the other synthetic proteins in that it contains one pentacoordinate, high-spin and one hexacoordinate, low-spin heme rather than two hexacoordinate low-spin cofactors. The open coordination site on the high-spin heme is inaccessible to exogenous imidazole but readily binds cyanide, suggesting that the α-helix containing the unbound histidine is nearby and partially shields the coordination site. The high-spin heme converts to low-spin at low-temperature, presumably via binding of the histidine residue on this nearby α-helix. It is suggested that the different behavior observed for the PHs protein is due to the fact that this heme is symmetric with respect to rotation about the α,γ-axis of the macrocycle which bisects the *meso*-carbons between the vinyl groups and propionic acid residues. This symmetry precludes rotational isomerism about the α,γ-axis to establish an unhindered fit. In contrast, all the other hemes examined contain at least one substituent smaller than a vinyl group which together with the fact that two different α,γ-rotational isomers are possible for each heme in the dimer could allow these hemes to avoid the like-substituent−like-substituent heme−heme interactions of PHs. The propensity to avoid such interactions could explain the inequivalent binding properties of the two hemes in the dimer. For the PHs protein wherein these interactions cannot be mitigated by rotation of the heme, other rearrangements of the protein must occur. These rearrangements could force the second-bound heme to assume a high-spin configuration.

Proteins containing tetrapyrrolic cofactors [hemes, (bacterio)chlorophylls, and related ring systems] perform a wide variety of tasks in nature including oxygen binding and transport, electron transfer, energy transfer, and catalysis (Dolphin, 1979; Scheer, 1991). Over the years, various approaches have been taken in attempts to prepare model systems which exhibit structural, electronic, and/or functional properties similar to those of the natural systems (Collman, 1977; Chang, 1982; Wasielewski, 1992; Ibers & Jameson, 1994; Ungashe & Groves, 1994). The ultimate utility of any model is determined by its ability to faithfully mimic the salient characteristics of the natural system. In the case of heme proteins, iron porphyrins in solution seldom accomplish this goal because the solvent cannot mimic the specialized, heterogeneous environment provided by the protein matrix.

† This work was supported by NIH Grants GM36243 (D.F.B.), GM41048 and GM48130 (P.L.D.), and HL22252 (K.M.S.).

‡ University of California, Riverside.

§ University of Pennsylvania.

|| Present address: Recombinant BioCatalysis, 512 Elmwood Ave., Sharon Hill, PA 19079.

⊥ University of California, Davis.

Present address: Department of Radiation Biology, Division of Radiation Medicine, Roswell Park Cancer Institute, Buffalo, NY 14236.

⊗ Abstract published in *Advance ACS Abstracts,* March 1, 1996.

0006-2960/96/0435-3429$12.00/0

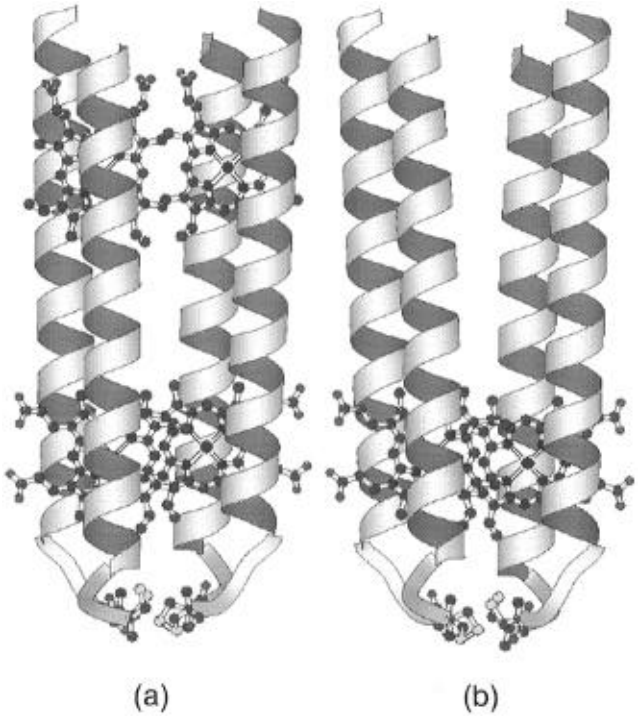

FIGURE 1: Schematic representation of (a) the cytochrome *b* maquette and (b) the diheme binding variant examined here.

As a consequence, efforts were directed early on toward the preparation of more elaborate synthetic architectures which incorporate structural elements intended to mimic the protein environment surrounding the heme active site (Collman, 1977; Chang, 1982). Recently, significant advances in *de novo* peptide synthesis have opened new directions in the construction of working models for proteins (DeGrado et al., 1989, 1991; Ghadiri & Fernholtz, 1990; Hecht et al., 1990; Regan & Clarke, 1990; Lieberman & Sasaki, 1991; Ghadiri et al., 1992a,b; Ghadiri & Case, 1993; Betz et al., 1993; Handel et al., 1993). These techniques have allowed the preparation of peptide-based macromolecular architectures which incorporate biological redox sites such as heme groups (Sasaki & Kaiser, 1989; Choma et al., 1994; Robertson et al., 1994). The availability of these synthetic proteins affords the opportunity to explore the molecular engineering in their assembly and to establish the minimal requirements for the function of their more complex natural counterparts.

As a first step toward the construction of small working models for redox proteins, one of our groups recently reported the preparation and properties of a water-soluble 124-residue four-helix bundle protein comprised of two identical, two-fold symmetric 62-residue di-α-helical peptide units that bind up to four heme groups (Robertson et al., 1994). The synthetic peptide was modeled to incorporate features of the heme-binding region of the diheme cytochrome *b* subunit of cytochrome bc_1 (Saraste 1984; Crofts et al., 1987; Howell & Gilbert, 1987; Yun et al., 1991). A schematic representation of the synthetic four-helix bundle protein, designated the cytochrome *b* maquette, is shown in Figure 1a. Robertson et al. (1994) considered that the two di-α-helical units were positioned parallel to each other so that the hemes liganded to histidines at 10,10′ and 24,24′ of one unit were paired with like hemes in the other unit. Recent work, in which a single coporphyrin appended to each di-α-helix at the terminal cysteine position was shown to form a cofacial dimer in the four-helix bundle, strongly supports the all parallel structure of Figure 1a (Rabanal et al., 1995). Despite the two-fold axis of symmetry between the two di-α-helical units, the electrochemical properties of the hemes in either pair are markedly different. It is not clear whether the redox inequivalence is derived purely from electronic interactions between the hemes or whether structural and/or environmental differences between the cofactors play an important role. In order to address these issues, we undertook a detailed spectroscopic [absorption, resonance Raman (RR),[1] electron paramagnetic (EPR) resonance] study of the heme groups in one of the simpler variants of the cytochrome *b* maquette characterized by Robertson et al. (1994). This synthetic protein, which is shown schematically in Figure 1b, contains an alanine at position 24 rather than histidine; consequently, only a single heme is bound per di-α-helical unit (Robertson et al., 1994). The redox potentials of the two hemes in this four-helix bundle are inequivalent (−100 and −215 mV) and of comparable magnitude to those observed for the two 10,10′ hemes of the cytochrome *b* maquette (−130 and −230 mV). The similarity of the redox potentials of the 10,10′ hemes in the two synthetic proteins suggests that the structures and/or environments of the cofactors are similar. However, the presence of two versus four hemes greatly simplifies the interpretation of the spectra.

The focus of the present investigation is the RR studies because the frequencies of the vibrational modes of the heme cofactor are extremely sensitive to the structure of the macrocycle and the effects of interactions with the protein matrix (Spiro 1983, 1988; Kitagawa & Ozaki, 1987; Schick & Bocian, 1987; Procyk & Bocian, 1992). In order to further investigate the properties of the heme cofactors in the synthetic protein, studies were conducted on peptides reconstituted with a number of different hemes in addition to protoheme IX (PHa). The structures of these hemes are shown in Figure 2 and include 2-vinyldeuteroheme IX (2-VDH), 4-vinyldeuteroheme (4-VDH), protoheme III (PHs), and 1-methyl-2-oxomesoheme XIII (2-OMH). The two monovinylhemes were examined because they afford the opportunity for selectively probing the environment around the two inequivalent vinyl groups at the 2- and 4-positions (Gersonde et al., 1989). PHs was examined because the disposition of the vinyl groups imparts approximate C_2 symmetry to the cofactor. This symmetry is absent in PHa due to the asymmetric disposition of the vinyl groups. 2-OMH was chosen for study because the oxo group can serve as a monitor of hydrogen bonding interactions and the dielectric properties of the surrounding medium (Babcock, 1988; Lutz & Robert, 1988; Krawczyk, 1989; Palaniappan & Bocian, 1995). Collectively, the studies of the various synthetic heme proteins provide a clearer picture of the structural and electronic properties of the heme cofactors and the nature of the protein environment surrounding these groups.

[1] Abbreviations: CCD, charge-coupled device; DMSO, dimethyl sulfoxide; EPR, electron paramagnetic resonance; Im, imidazole; 2-MeIm, 2-methylimidazole; 2-OMH, 1-methyl-2-oxomesoheme XIII; PHs, protoheme III; PHa, protoheme IX; RR, resonance Raman; Tris, tris(hydroxymethyl)aminomethane; 2-VDH, 2-vinyldeuteroheme IX; 4-VDH, 4-vinyldeuteroheme IX.

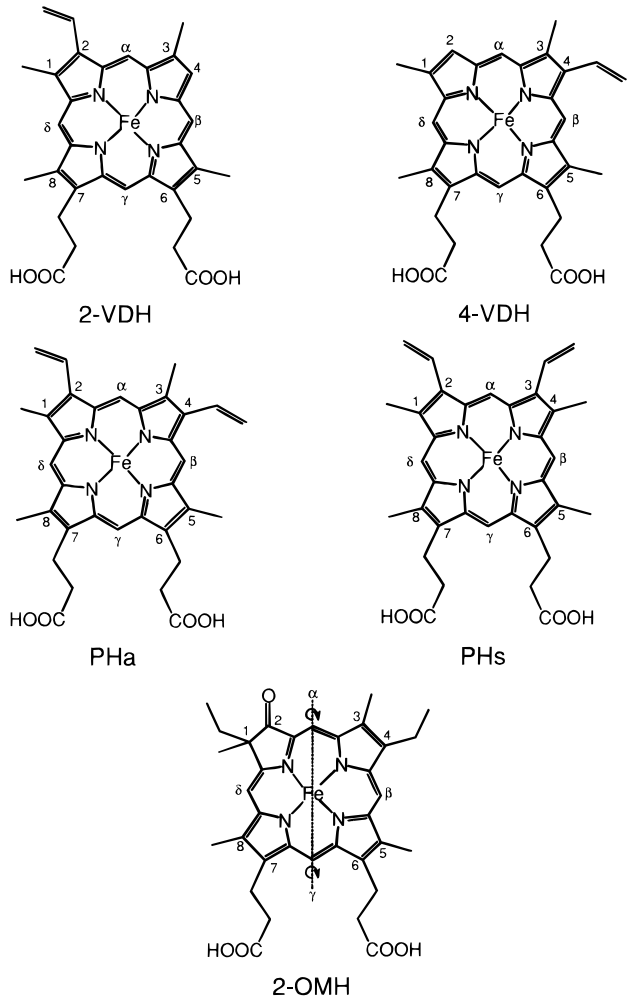

FIGURE 2: Structures of the various hemes used in this study. The location of the α,γ-axis is shown for 2-OMH.

MATERIALS AND METHODS

PHa chloride was purchased from Porphyrin Products (Logan, UT) and used as received. The chloride salts of 2-VDH, 4-VDH, PHs, and 2-OMH were synthesized by literature methods (Chang & Wu, 1986; Smith et al., 1983, 1986). Their purity was >99% as judged by spectral and chemical analysis. The 62-residue di-α-helical H10,10′A24,24′ peptide was synthesized and purified and the various hemes were incorporated as described by Robertson et al. (1994). Binding of the hemes to the peptide (in 50 mM Tris, pH 8.0, 100 mM NaCl) was monitored optically as described by these workers. The organic solvents used for the absorption and RR studies [CH_2Cl_2, acetone, and dimethyl sulfoxide (DMSO)] were all spectroscopic grade (Aldrich). These solvents and the detergent Triton X-100 (Aldrich) were used as received. Aqueous solutions of the various hemes were prepared in deionized water at pH 8.2. Imidazole (Im) and 2-methylimidazole (2-MeIm) (both Aldrich) were recrystallized three times from benzene. The low-spin bis-Im and high-spin 2-MeIm complexes of the various hemes in solution were prepared by adding an excess of the ligand to a solution containing the hemin chloride. The ferrous proteins and ferrous complexes in solution were prepared by adding a small excess of freshly prepared $Na_2S_2O_4$ in buffer or a DMSO/buffer mixture. In the case of the PHs protein, reduction with $Na_2S_2O_4$ resulted in a small, but noticable, amount of protein denaturation (as evidenced by precipitate formation and the appearance of Soret features characteristic of free heme in solution). Consequently, all the spectroscopic studies on the ferrous PHs protein were conducted on samples reduced with ascorbate under illumination. No denaturation was detected under these condions.

The absorption spectra obtained for the assessment of heme binding to the peptide were recorded using a scanning or diode array spectrophotometer (Perkin-Elmer Lambda-2 or Hewlett-Packard 8452A). The absorption spectra of the synthetic proteins were recorded both before and after the RR studies to order to confirm the integrity of proteins. These measurements indicated that all the proteins were stable under laser irradiation.

The RR spectra were acquired with a triple spectrograph (Spex 1877) equipped with a holographically etched 2400 groove/mm grating in the final stage. The scattering was collected at 90° to the incident laser beam by use of a camera lens (Canon 50 mm f/1.2). The excitation wavelengths were provided by the outputs of a Kr ion laser (Coherent Innova 200-K3). A 1152 × 298 pixel, front-illuminated, UV-enhanced charge-coupled device (CCD) was used as the detector (Princeton Instruments, LN/CCD equipped with a EEV 1152-UV chip). The laser powers were typically 5 mW. The frequencies were calibrated using the known frequencies of indene. The frequencies are accurate to ±1 cm^{-1} for strong and/or isolated bands. The slit widths were set to provide ∼2 cm^{-1} resolution.

The electron paramagnetic resonance (EPR) spectra were recorded with an X-band spectrometer (Bruker ER200D) equipped with an NMR gauss meter (Bruker ER035M) and a microwave frequency counter (Hewlett-Packard 3550B). Temperature control was achieved with a liquid He cryostat (Oxford ESR-9).

RESULTS

Heme Binding. Titration of the various hemes into solutions containing the apoprotein indicated that all of the complexes were incorporated into the protein. The K_D values determined for 2-VDH, 4-VDH, PHs, and 2-OMH were comparable to one another and similar to those previously measured for PHa (Robertson et al., 1994). As is the case for the latter heme, two K_D values are resolved for each of the other complexes, indicative of negative binding cooperativity in the two sites of the four-helix bundle. The two K_D values for all the complexes were typically ≤0.05 μM and ∼1 μM.

Absorption Spectra. The absorption spectra of the ferric and ferrous forms of the synthetic heme proteins are shown in Figures 3 and 4, respectively. With the exception of the PHs protein, the spectra of all the other synthetic proteins are essentially identical to those of the bis-Im complexes of the ferric and ferrous forms of the hemes in solution (not shown). These spectral characteristics indicate that 2-VDH, 4-VDH, and 2-OMH form low-spin, bis-ligated complexes with the protein as has been previously determined for PHa (Robertson et al., 1994). The absorption spectra of both the ferric and ferrous forms of the PHs protein are qualitatively different from those of the other synthetic vinylheme proteins. In the case of the ferric form, the Soret band is distinctly broader and exhibits a shoulder on the blue side. In the visible region, the lowest energy feature of the PHs

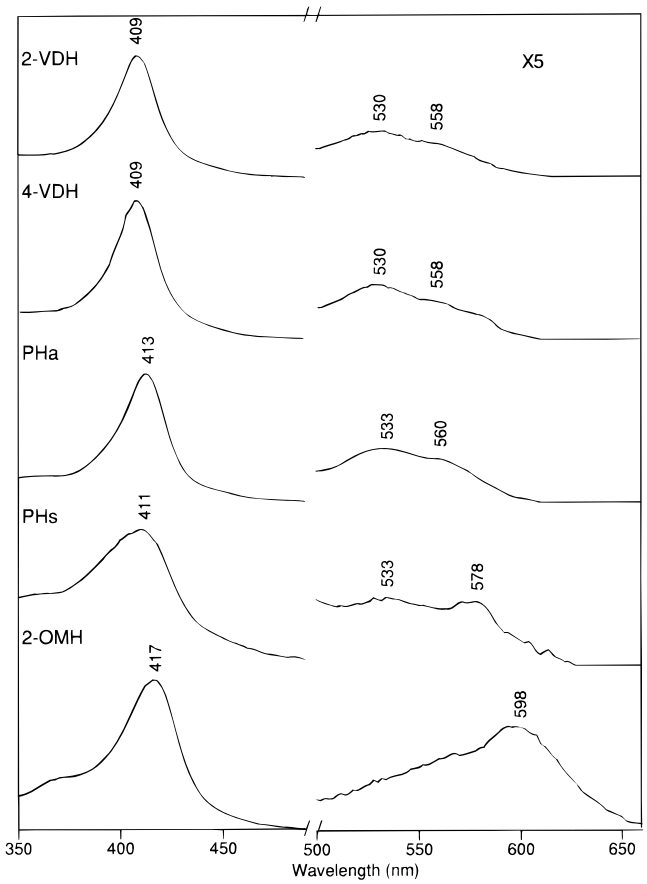

FIGURE 3: Absorption spectra of the ferric forms of the synthetic heme proteins.

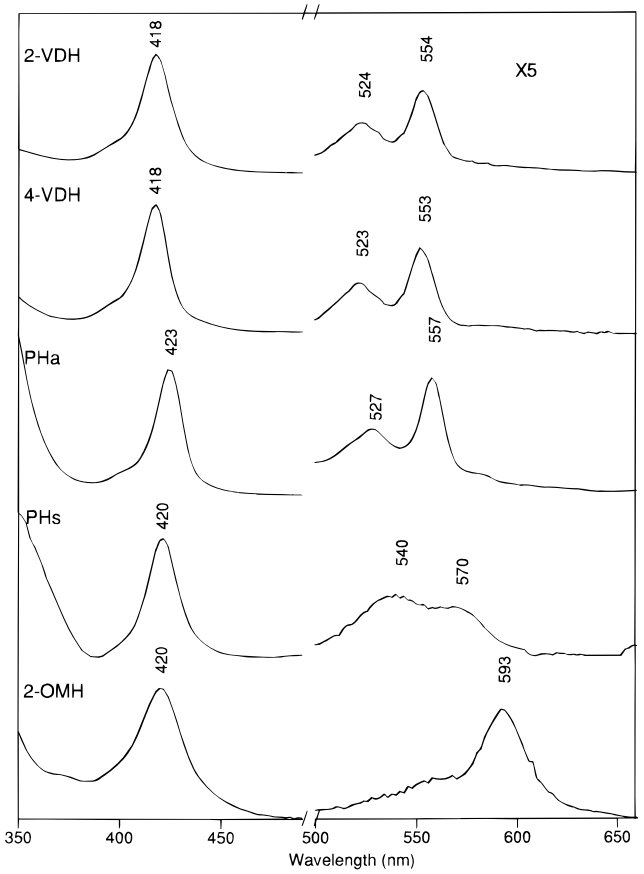

FIGURE 4: Absorption spectra of the ferrous forms of the synthetic heme proteins.

protein is significantly to the red (~578 nm) of that of the other vinylheme proteins (~558 nm). In the ferrous form, the visible region absorption differences observed for the PHs protein versus other the vinylheme proteins are even more pronounced. Here, the PHs protein exhibits two broad, poorly resolved features at 570 and 540 nm compared with the clearly resolved bands observed at ~555 and ~525 nm for the other vinylheme proteins. In contrast, the Soret absorption band of the ferrous PHs protein is quite similar to that of the other ferrous vinylheme proteins.

The general appearance of the absorption spectra of the PHs protein suggests that some component of high-spin heme is present (Adar, 1978; Churg & Makinen, 1983). This assessment is clearly confirmed by the RR scattering characteristics of the protein (vide infra). In order to investigate the possible origins of the high-spin contribution, various other experiments were performed on the PHs protein. These experiments are described in more detail below.

(1) Absorption spectra of the PHs protein were examined after a small amount (0.1%) of detergent (Triton X-100) was added to the solution. The presence of detergent had no effect on the spectrum of either the ferric or ferrous forms of the protein. This result can be contrasted with that observed for free heme in solution. Free heme is strongly aggregated at the working pH (8.0). Addition of detergent breaks up the aggregate and significantly alters the absorption spectrum. The observation that detergent has no effect on the absorption spectrum of the PHs protein indicates that the high-spin heme is bound to the synthetic protein and is not due to heme in solution.

(2) Absorption spectra of the PHs protein were examined after excess Im and KCN were added to the solutions. The addition of Im has no effect on the spectra of either the ferric or ferrous forms the protein. In contrast, the addition of KCN to ferric PHs results in a narrowing and red shift of the Soret band (to 427 nm), consistent with conversion to an all low-spin species (Adar, 1978; Makinen & Churg, 1983). [The effect of KCN on the ferrous PHs protein was not investigated.] The position and shape of the Soret band further indicates that CN^- replaces one of the two histidine ligands on the low-spin heme. This behavior is also observed for the other vinylheme proteins wherein addition of KCN shifts the Soret band from ~412 to ~421 nm, indicative of replacement of one histidine on each low-spin heme by CN^-. The position of the Soret maximum of the ferric PHs protein (427 nm) is redder than that observed for the cyano forms of the other vinylheme proteins (421 nm) and reminiscent of that observed for ferric PHs$(CN)_2^-$ in solution (429 nm). Accordingly, we cannot rule out the possibility that addition of KCN pulls some of the heme out of the protein. [This could also occur in the other vinylheme proteins although to a smaller extent.] Regardless, the spectral features observed upon addition of Im and KCN indicate that the high-spin PHs cofactor in the synthetic protein is inaccessible to larger ligands such as Im but readily accessible to smaller ligands such as CN^-. It is plausible that the high-spin PHs cofactor does not bind relatively weak ligands, such as Im, because the cofactor is hexacoordinate. A solution water molecule could serve in this capacity. This possibility is excluded, however, by the results of the RR experiments which clearly indicate pentacoordinate, high-spin heme (vide infra).

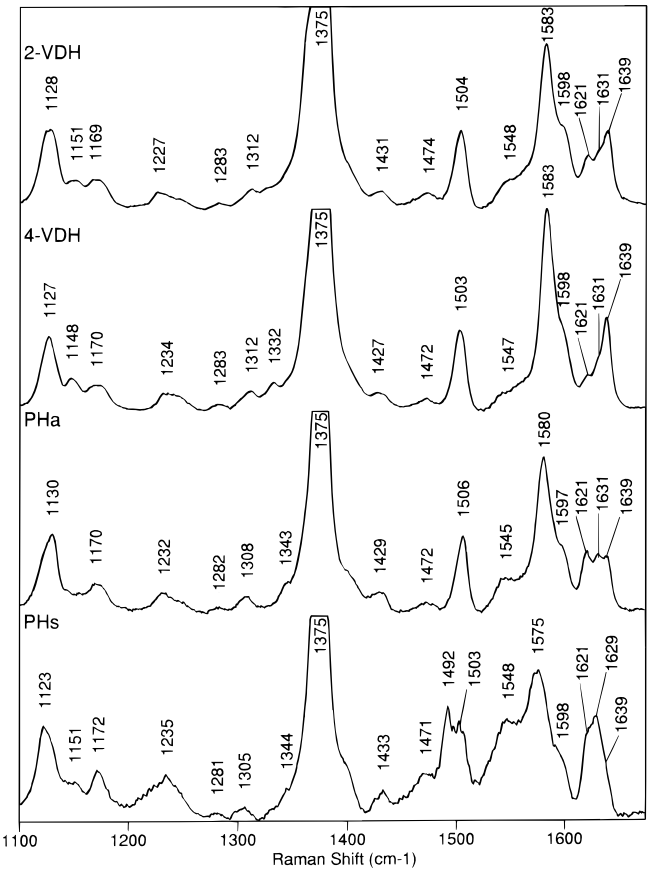

FIGURE 5: High-frequency regions of the Soret excitation (λ_{ex} = 413.1 nm) RR spectra of the ferric forms of the vinylheme proteins.

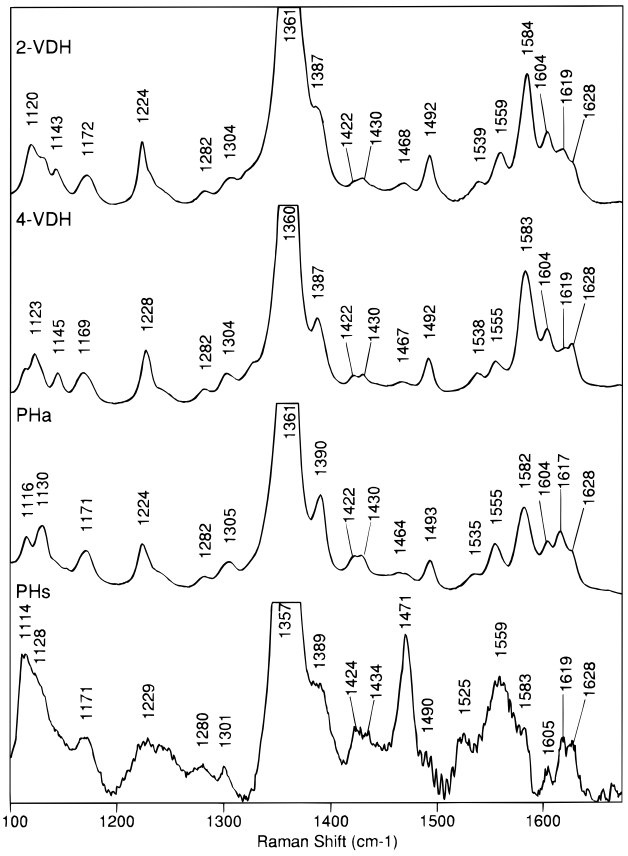

FIGURE 6: High-frequency regions of the Soret excitation (λ_{ex} = 415.4 nm) RR spectra of the ferrous forms of the vinylheme proteins.

(3) Attempts were made to simulate the absorption spectra of the PHs protein by summing the spectra observed for the low-spin PHs(Im)$_2$ and high-spin PHs(2-MeIm) complexes in solution. The spectrum of the ferric protein could be reproduced reasonably well by adding the solution spectra in an ~1:1 ratio. In contrast, the spectrum of the ferrous PHs protein could not be reproduced by this procedure.

RR Spectra. The high-frequency regions of the Soret-excitation RR spectra of the ferric and ferrous forms of the various vinylheme proteins are shown in Figures 5 and 6, respectively. The analogous RR spectra of the 2-OMH protein are shown in the top and bottom traces, respectively, of Figure 7. We first describe the RR scattering characteristics of the ring-skeletal modes of the various synthetic heme proteins. We then focus on the vinyl stretching vibrations, $\nu_{C=C}$, of the vinylheme proteins and the oxo-carbonyl stretching mode, $\nu_{C=O}$, of the 2-OMH protein.

(1) Ring-Skeletal Modes. The RR spectra of the 2-VDH, 4-VDH, PHa, and 2-OMH proteins are essentially identical to those of the bis-Im complexes of the ferric and ferrous forms of the hemes in solution (Kalsbeck et al., 1995; Kalsbeck and Bocian, unpublished results). This behavior parallels the absorption characteristics of these species. The spectra of the ferric vinyl proteins are characterized by strong polarized RR bands assigned to ν_2 (~1580 cm^{-1}), ν_3 (~1505 cm^{-1}), and ν_4 (1375 cm^{-1}), and a depolarized band assigned to ν_{10} (~1639 cm^{-1}) (Choi et al., 1982; Spiro, 1983). In the ferrous forms of the vinylheme proteins, these bands are shifted to approximately 1583, 1492, 1360, and 1619 cm^{-1}, respectively. In the case of the 2-OMH protein, all of the observed RR bands are polarized. In the ferric form, particularly strong features are observed at 1601, 1587, and 1374 cm^{-1}; in the ferrous form, the spectrum is dominated by a strong band at 1360 cm^{-1}. Specific assignments for the RR bands of the 2-OMH protein cannot be made because the vibrational spectra of oxoporphyrins have not yet been analyzed in detail. However, based on the frequency and iron oxidation-state sensitivity, the 1374-cm^{-1} (ferric)/1360-cm^{-1} (ferrous) bands appear to be analogs of the ν_4 band of iron porphyrins.

A key feature in the RR spectra of both the ferric and ferrous forms of the 2-VDH, 4-VDH, PHa, and 2-OMH proteins is that the number of bands observed is that expected for *single* heme group. There is no evidence for any broadening or splitting of any of the bands. These results indicate that any differences in the ring-skeletal-mode frequencies of the two heme cofactors in the four-helix bundle are far smaller than the widths of the RR bands. This in turn indicates that the structures of the hemes are essentially identical.

The RR spectra of the ferric and ferrous forms of the PHs protein are distinctly different from those of the other vinylheme proteins. This behavior parallels the absorption characteristics of the former versus latter proteins. In the ferric PHs protein, polarized RR bands assignable to ν_3 are observed at both 1503 and 1492 cm^{-1} (Figure 5, bottom trace). As is the case for the other vinylheme proteins, the former band is due to a hexacoordinate, low-spin heme. The frequency of the latter band is an unambiguous signature for a high-spin, pentacoordinate vinylheme (Choi et al., 1982; Spiro, 1983, 1988). In hexacoordinate, high-spin ferric complexes, ν_3 occurs near 1480 cm^{-1}. The presence of both high-spin, pentacoordinate and low-spin, hexacoordinate

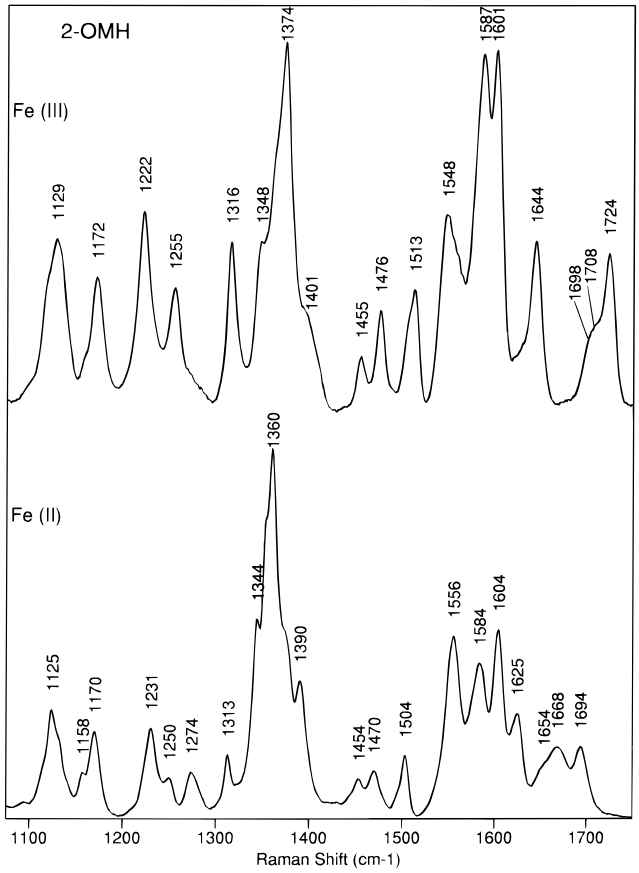

FIGURE 7: High-frequency regions of the Soret excitation RR spectra of the ferric (top trace; $\lambda_{ex} = 413.1$ nm) and ferrous (bottom trace; $\lambda_{ex} = 415.4$ nm) forms of the 2-OMH protein.

heme is also reflected in the spectral signatures of the PHs protein in the regions of the ν_2 and ν_{10} bands. In the ν_2 region, a broad envelope of bands is observed which maximizes near 1575 cm^{-1}. This envelope is attributed to the superposition of the ν_2 bands of the two types of hemes which are expected near ~1570 (high-spin-5c) and 1580 cm^{-1} (low-spin-6c) (Choi et al., 1982; Spiro, 1983). In the ν_{10} region, a strong band is observed near 1629 cm^{-1} with a shoulder to the higher frequency side. Again, these features are attributed to the superposition of the ν_{10} bands of the two types of hemes which are expected near 1626 (high-spin-5c) and 1640 cm^{-1} (low-spin-6c). [The $\nu_{C=C}$ modes also contribute to the 1629-cm^{-1} band (vide infra).]

The differences between the RR spectra of the ferrous PHs protein and the those of the other ferrous vinylheme proteins are most apparent in the region of the ν_2 and ν_3 modes. In the case of the ν_3 modes, a strong band is observed at 1471 cm^{-1}, characteristic of a high-spin, pentacoodinate vinylheme (Choi et al., 1982; Spiro, 1983). The ν_3 band of the low-spin, hexacoordinate vinylheme is observed as a shoulder on the latter band at ~1490 cm^{-1}. The ν_2 mode of the high-spin vinylheme is observed near 1559 cm^{-1}; the analogous mode of the low-spin vinylheme occurs as a shoulder near 1583 cm^{-1}. [The 1583 cm^{-1} band may also contain some contribution from the ν_{37} band of the high-spin, pentacoordinate vinylheme (Choi et al., 1982; Spiro, 1983).] The assignments of the ν_{10} bands of both the high- and low-spin hemes are complicated by interference with other modes. These ν_{10} bands are expected near 1604 and 1619 cm^{-1}, respectively, consistent with the frequencies of two observed bands. However, the ν_{37} band of the low-spin heme is also expected near 1604 cm^{-1}, whereas $\nu_{C=C}$ modes of both hemes are expected near 1620 cm^{-1} (vide infra).

In order to obtain an estimate of the relative contributions of the high- and low-spin hemes to the RR spectra of the PHs protein, the spectra were simulated by summing the spectra of the PHs$(Im)_2$ and PHs(2-MeIm) complexes in solution. In the case of the ferric protein, this procedure could be performed with some confidence because the absorption spectrum of this species is fairly well reproduced by a superposition of the spectra of the free PHs complexes in solution (vide supra). This allows scaling the RR intensities to account for the differences in cross section of the high- and low-spin species. The simulations reveal that the RR spectrum of the ferric PHs protein can be reproduced by adding the solution spectra in an ~1:1 ratio, as was the case for the absorption spectrum (vide supra). Reliable simulations of the RR spectrum of the ferrous PHs protein are not possible because the absorption spectrum of this species cannot be simulated by a superposition of the absorption spectra of the high- and low-spin complexes in solution. Without knowledge of the exact positions of the Soret maxima of the high- and low-spin hemes in the protein, the RR intensities cannot be accurately scaled to account for differences in the cross sections of the two types of complexes.

(2) $\nu_{C=C}$ Modes. The $\nu_{C=C}$ modes of vinylhemes occur in the 1620−1630-cm^{-1} region and are nearly independent of the oxidation- and spin-state of the iron ion (Choi et al., 1982; Spiro, 1983; Kalsbeck et al., 1995). Inspection of the RR spectra of the ferric forms of the various vinylheme proteins (Figure 5) reveals that two $\nu_{C=C}$ modes are clearly observed for the 2-VDH, 4-VDH, and PHa proteins (~1621 and ~1631 cm^{-1}). In the case of the ferric PHs protein, it appears that two $\nu_{C=C}$ modes are also present in the 1620−1630-cm^{-1} region; however, this interpretation is not certain due to interference from the ν_{10} band of the high-spin species (vide supra). In the case of the ferrous forms of all four vinylheme proteins (Figure 6), interference from the ν_{10} band-(s) of the low-spin heme(s) precludes a definitive assignment of all the $\nu_{C=C}$ modes; however, the band observed near 1628 cm^{-1} is attributed to one of these modes.

The appearance of two $\nu_{C=C}$ modes at ~1621 and ~1631 cm^{-1} in the RR spectra of the vinylheme proteins, *including the two bands observed for the monovinylheme proteins*, parallels the behavior observed for the various vinylhemes in solution (Kalsbeck et al., 1995). This is illustrated in Figure 8 (left panel), which compares the RR spectrum of the ferric PHa protein in the region of the $\nu_{C=C}$ modes with those of the PHa$(Im)_2^+$ in several different solvents. Inspection of these data reveals that the general shape of the $\nu_{C=C}$ band envelope of PHa in the protein is more similar to that observed for a monomeric free heme (DMSO, CH_2Cl_2, water + Triton X100) than a heme aggregate (water). This is also the case for the other vinylheme proteins (not shown). The general spectral characteristics of the $\nu_{C=C}$ modes of the different vinylheme proteins suggest that the protein environment in the region of the vinyl groups is qualitatively similar for all the synthetic proteins. [The PHs protein could be an exception (vide infra).]

(3) $\nu_{C=O}$ Mode. The $\nu_{C=O}$ mode of 2-OMH is expected in the 1680−1750-cm^{-1} region (Ching et al., 1982; Andersson et al., 1990; Mylrajan et al., 1991). The exact frequency of this mode is expected to be sensitive to a variety of factors

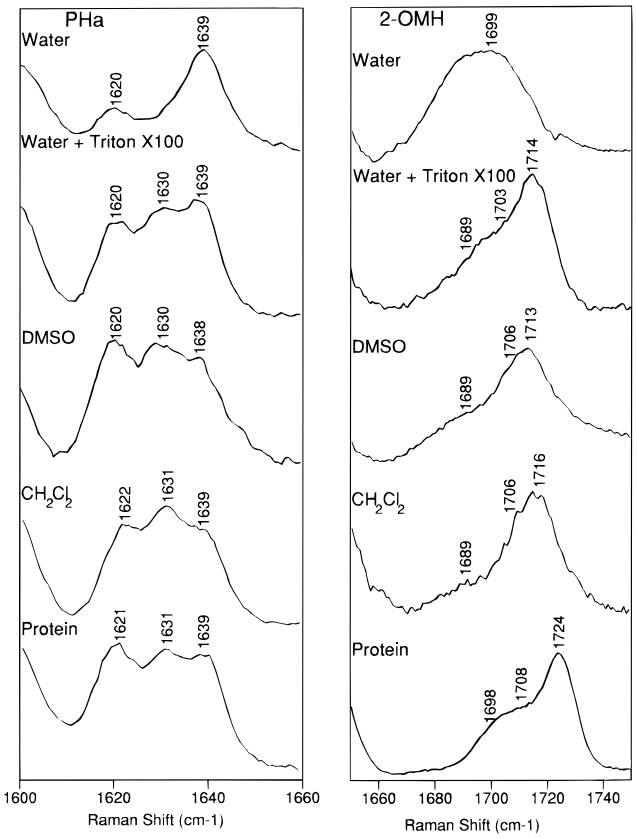

FIGURE 8: Soret excitation (λ_{ex} = 413.1 nm) RR spectra of ferric PHa (left panel) and 2-OMH (right panel) in the synthetic protein and in various solvents. The spectral regions shown focus on the $\nu_{C=C}$ modes of PHa and the $\nu_{C=O}$ mode of 2-OMH.

such as the oxidation-state of the iron ion, the hydrogen bonding, and the dielectric properties of the host medium (Babcock, 1988; Lutz & Robert, 1988; Krawczyk, 1989; Palaniappan & Bocian, 1995). Regardless, the $\nu_{C=O}$ mode is expected be the highest frequency fundamental mode in the RR spectrum (excluding C−H stretches). Accordingly, the most reasonable candidates for the $\nu_{C=O}$ modes of the ferric and ferrous forms of the 2-OMH proteins are the bands observed at 1724 and 1694 cm^{-1}, respectively (Figure 7). Additional features are observed on the low-frequency side of both of these bands (at ∼1700 and ∼1668 cm^{-1}, respectively) which could also be due to $\nu_{C=O}$ modes. This would signal a fairly inhomogeneous environment for the oxo group. However, the ∼1700- and ∼1668-cm^{-1} features are also observed in the RR spectra of monomeric 2-OMH-$(Im)_2^+$ in solution. This is illustrated in Figure 8 (right panel) which compares the RR spectrum of the ferric 2-OMH protein in the region of the $\nu_{C=O}$ mode with those of the 2-OMH$(Im)_2^+$ in several different solvents. The presence the additional modes in the solution spectra of the complex strongly suggests that they are not $\nu_{C=O}$ modes. Given this, the 1724- and 1694-cm^{-1} modes of the ferric and ferrous PHs proteins would be attributed to superpositions of the bands of the oxo groups of the two hemes in the the four-helix bundle. This observation indicates that the two oxo groups are in similar protein environments.

Inspection of the RR data shown in Figure 8 (right panel) reveals that the frequency of the $\nu_{C=O}$ mode of the 2-OMH protein is distinctly higher than that observed for any of the solvents. The spectra of the protein are qualitatively and quantitatively different from those of 2-OMH$(Im)_2^+$ in water (top trace). In this solvent, the $\nu_{C=O}$ band is extremely broad (∼40 cm^{-1}) and centered below 1700 cm^{-1}. The general appearance of the $\nu_{C=O}$ band most likely arises from a combination of heme aggregation and solvent hydrogen bonding to the oxo group (Lutz & Robert, 1988; Babcock, 1988). Dispersion of the aggregate with detergent results in a much narrower $\nu_{C=O}$ band centered near 1714 cm^{-1} (second trace). The presence of the detergent may also screen the oxo group from the solvent and prevent hydrogen bonding. The vibrational characteristics of the $\nu_{C=O}$ mode in the 2-OMH protein indicate that the oxo groups of both hemes in the four-helix bundle are free from hydrogen bonds and in an environment very different from that of a water solution. The fact that the frequency the $\nu_{C=O}$ mode of the hemes in the protein is ∼8−10 cm^{-1} higher than that observed for the mode in any of the organic solvents examined further suggests that the protein environment is also different from that of the organic solvents. In particular, it is known that the frequency of the $\nu_{C=O}$ mode is inversely proportional to the effective dielectric constant of the medium (Krawczyk, 1989). Accordingly, the relatively high $\nu_{C=O}$ frequency observed for the 2-OMH protein indicates that the oxo groups reside in a region of very low effective dielectric constant.

EPR Spectra. The EPR spectra of the ferric forms of the all the synthetic heme proteins were examined in the temperature range 5−20 K (not shown). The spectra of all the proteins exhibit rhombic signals characteristic of low-spin heme (Palmer, 1983). In the case of the vinylheme proteins, the *g* values are very similar those previously reported for the ferric cytochrome *b* maquette (g_z, g_y, g_x = 2.89, 2.24, 1.54, respectively) (Robertson et al., 1994). The *g* values for the ferric 2-OMH protein are somewhat different (g_z, g_y, g_x = 2.90, 2.37, 1.73, respectively). The only remarkable feature of the EPR spectra is that no signals characteristic of a high-spin heme are observed for the ferric PHs protein. These signals should be readily observable considering that both the absorption and RR spectra suggest a 1:1 ratio of high- and low-spin heme and that certain *g* values characteristic of the two types of heme are very different (Palmer, 1983). It should be noted, however, that the absorption and RR spectra were recorded at ambient temperature, whereas the EPR spectra were obtained at very low temperature. The absence of EPR signals due to a high-spin heme suggests that this cofactor becomes low spin at low temperature. In order to investigate this possibility, we attempted to obtain low-temperature RR spectra of the ferric 2-OMH protein. These studies were inconclusive, however, because the RR scattering characteristics of the frozen solutions were extremely poor.

DISCUSSION

The spectroscopic data reported herein serve as benchmarks for formulating a self-consistent model for the structure of the synthetic heme protein and for delineating the salient features which influence the physicochemical properties of the cofactors. A particularly important characteristic which emerges is that the two electrochemically inequivalent hemes in the four-helix bundle have essentially identical structures and ring conformations. The PHs protein is a clear exception and will be discussed later. Thus, the cooperative redox behavior observed for the cofactors must arise from either electronic interactions between the two

hemes or from global asymmetries in the protein environment in the two halves of the dimer. We favor the former explanation for the following reason. The redox potentials of the two hemes in all the proteins are separated by at least 100 mV (Robertson et al., 1994; D. E. Robertson and P. L. Dutton, unpublished results). Redox difference of this magnitude would be expected if the two cofactors are within van der Waals distance with iron-to-iron separations in the range of 13 Å or less (Gunner & Honig, 1991). This type of heme arrangement is consistent with the minimum energy structures calculated for the four-helix bundle (D. E. Robertson and P. L. Dutton, unpublished results). In order for the protein environment alone to generate a redox difference of the magnitude observed (∼100 mV or 2 kcal/mol), the bonding interactions/electric fields and/or dielectric properties in the region of the two hemes must be quite different. Such differences should be reflected in the vibrational characteristics of the peripheral substituents, and it is clear that this is not the case. For example, the oxo groups of the two hemes in the 2-OMH protein have nearly identical vibrational frequencies.

The vibrational characteristics of the oxo group of the 2-OMH protein provide additional insights into the explicit geometrical arrangement of the two hemes in the four-helix bundle. In particular, the oxo group spectra indicate that they are buried deep within a region of low effective dielectric constant. The region which best meets this criterion is the hydrophobic interface between the two units which form the four-helix bundle. This region is comprised predominantly of apolar leucine residues which were designed into the peptide to stabilize helix−helix interactions. The fact that the oxo groups are free of hydrogen bonds further indicates that the helix−helix interactions are sufficiently strong to exclude intrusion of even a minimal amount of water. All of these features are accommodated by a model in which the two heme macrocycles are in an approximate coplanar arrangement with the 2,3-position edges (see Figure 2) in contact in the interior of the four helices and the propionic acid side chains of both directed outward toward the hydrophilic regions of the dimer and into the solvent. This geometrical arrangement of the hemes is qualitatively consistent with that we originally suggested (Robertson et al., 1994; Figure 4a). The relatively tight interior cavity formed by the hemes further suggests that the planes of the two macrocycles cannot be in a direct head-to-head arrangement but rather must be slipped somewhat with respect to one another as shown in Figure 1.

The vibrational characteristics of the vinyl groups in the vinylheme proteins provide another measure of the environment in this region of the heme cofactors. The important observation is that two $\nu_{C=C}$ modes are observed for all of the proteins including the monovinylheme systems. [This is clearly the case for the 2-VDH, 4-VDH, and PHa proteins, but not certain for the PHs protein.] It is conceivable that multiple $\nu_{C=C}$ modes occur because the two hemes in the dimer directly interact with one another. Such interactions are particularly plausible for the groups at the 2- and 3-position if the hemes are in a direct (rather than slipped) edge-to-edge arrangement. It is also possible that the multiple $\nu_{C=C}$ modes are due to inequivalences in the protein environment around the substituents at the different positions on the ring. The doubling observed for the $\nu_{C=C}$ modes of various natural PHa containing proteins and for certain proteins reconstituted with 2-VDH and 4-VDH has been ascribed to environmental inequivalences (Terner & Reed, 1984; Gersonde et al., 1989; Hildebrant et al., 1989, 1994; Smulevich at al., 1991). In the case of the monovinylheme and PHa proteins, the environment around a particular substituent could also be affected by heme rotational isomerism similar to that observed for heme reconstituted myoglobins (La Mar et al., 1978, 1983, 1984; Miki et al., 1981; Docherty & Brown, 1982; Ahmad & Kincaid, 1983; Jue et al., 1983; Lecomte et al., 1985; Atamian & Bocian, 1987). The isomers are generated by a 180° rotation of the heme about the α,γ-axis which runs through the *meso*-carbon atom between the two propionic acid groups (see Figure 2). The vinyl group(s) of 2-VDH, 4-VDH, and PHa would reside in a different protein environment in the two orientational isomers because the α,γ-axis of the heme is perpendicular to the C_2 axis of the four-helix bundle. However, these orientational isomers cannot occur for PHs because the 2- and 3-vinyls are equivalent.

The large number of factors which could contribute to the appearance of multiple $\nu_{C=C}$ modes for the vinylheme proteins renders an exact interpretation difficult. Nevertheless, a key observation is that for the 2-VDH, 4-VDH, and PHa proteins, only two $\nu_{C=C}$ modes are observed whose frequencies and intensities are similar to those observed for these vinylhemes in solution (Figure 8; Kalsbeck et al., 1995). The fact that vinylhemes in solution, including monovinyl species, exhibit two $\nu_{C=C}$ modes has only recently been recognized. In a detailed RR study of vinylhemes, we have shown the two $\nu_{C=C}$ modes arise from two nearly equal-energy vinyl torsional conformers which are intrinsic to a single vinyl group (Kalsbeck et al., 1995). The 1621- and 1631-cm^{-1} $\nu_{C=C}$ modes are assigned to torsional isomers in which the vinyl group points toward the β-pyrrole methyl group and *meso*-hydrogens, respectively. In the case of divinylhemes, such as PHa and PHs, each vinyl group contributes a band at each frequency; however, the bands are not resolved. Instead the intensity of both $\nu_{C=C}$ modes of the divinylhemes is approximately twice that of the monovinylhemes.

The fact that the spectral characteristics of the $\nu_{C=C}$ modes of the 2-VDH, 4-VDH, and PHa proteins are essentially identical to those of the hemes in solution strongly suggests that vinyl torsional isomerism is the origin of the multiple modes. In this scenario, the protein environment around any particular vinyl groups must be packed loosely enough that these substituents are free to assume the conformations preferred in solution. This would be the case regardless of whether the hemes in the proteins also exist as α,γ-rotational isomers. The torsional freedom exhibited by the vinyl groups in the 2-vinyl-3-methyl containing hemes (2-VDH and PHa) would seem to preclude any significant steric interactions between the hemes in the region of these substituents.

The most unexpected result of the current study is the observation that one of the hemes in the PHs protein is a pentacoordinate, high-spin species. The heme optical titration studies indicate that the 1:1 ratio of the two hemes is due one low- and one high-spin heme per four-helix bundle, the former being the most tightly bound, rather than a statistical distribution of low- and high-spin forms which averages to a 1:1 ratio. Given this, it might have been expected that the K_D value for the high-spin heme would be different from those of the corresponding low-spin hemes

in the other proteins. Differences in K_D values on the order of 5-fold or less would be difficult to determine, however, because the absorption spectra of high-spin PHs in solution and both low- and high-spin PHs in the protein are severely overlapped. It is also possible that the K_D value of the second and not the first histidine ligand of the less tightly bound heme is perturbed in the PHs protein. If so, the measured K_D value for the high-spin heme in this protein and the less tightly bound low-spin hemes in the other proteins could be similar. [The individual K_D values for the two histidines are not resolved for any of the bis-ligated species.] In the case of the PHs protein, the binding of the second histidine which occurs at low temperatures suggests that the low-spin form is destabilized by only a few kcal/mol at ambient temperature. This observation is qualitatively consistent with a picture in which the α-helix containing the nonbinding histidine is in close proximity to the cofactor and can shield it from exogenous ligands such as Im.

PHs is the only heme thus far investigated which forms a high-spin cofactor in the synthetic proteins. The single structural characteristic which distinguishes this heme from all these others is the symmetrical disposition of the vinyl substituents about the α,γ-axis of the macrocycle. In a 2,3-position edge-to-edge arrangement of the cofactors, this symmetry precludes alleviating heme−heme interactions between like substituents on the two hemes in the four-helix bundle via rotation about the α,γ-axis. The propensity to avoid these interactions could explain the inequivalent binding properties of the two hemes in the dimer. In this scenario, an asymmetric heme, (2-VDH, 4-VDH, PHa, and 2-OMH) might bind with no particular preference for a particular rotational isomer. Binding of the second heme in the same rotational orientation might then be strongly discriminated against due to like-substituent−like-substituent interactions. These interactions might be partially, but not necessarily completely, eliminated via rotation of the second heme about the α,γ-axis. Thus, the preferred structure for the synthetic four-helix bundle would be a dimer wherein the two asymmetric hemes occupy different rotational isomers. In the case of the asymmetric vinylhemes, the substituent mismatch might allow the vinyl groups relative freedom to assume the torsional conforms preferred in solution. For the PHs protein, where these interactions cannot be mitigated by rotation of the heme, other rearrangements of the protein must occur. These rearrangements could force the second-bound heme to assume a high-spin configuration. The magnitude of the destabilization is not, however, large enough to preclude binding of the second heme or promote dissociation of the four-helix bundle. This view is also consistent with the relatively facile conversion of the second binding heme from high- to low-spin at low temperature. If like-substituent−like-substituent interactions do influence heme binding in the PHs protein, it might be expected that the $\nu_{C=C}$ modes of the cofactor would be perturbed. Unfortunately, interference from the ν_{10} skeletal mode of the high-spin species prevents a detailed analysis of the vibrational characteristics of the $\nu_{C=C}$ modes of the PHs protein (vide supra). This problem could be avoided by using a symmetrical heme whose reporter group frequency falls outside the region of the ring-skeletal modes. A symmetrical dioxo complex would be a good candidate and will be the target of future studies.

CONCLUSIONS AND PROSPECTS

The studies reported herein resolve many issues concerning the detailed structural features of the synthetic heme protein and provide reasonable explanations for the unique physicochemical properties of the system. Many of the structural characteristics originally suggested for the protein on the basis of intuition have been borne out by the present studies. The properties delineated for the prototypical synthetic cytochromes also provide insights into future design strategies. In particular, they suggest methods for obtaining proteins containing high-spin hemes and/or open coordination sites. These structural motifs are required for the construction of viable synthetic models for more complex redox/catalytic proteins such as cytochrome *c* oxidase. The studies reported herein represent only an initial effort into the elucidation of the factors which control heme structure and ligation state in multi-heme synthetic cytochromes. These factors can only be determined by detailed studies of synthetic proteins reconstituted with other types of heme cofactors and/or comprised of altered primary amino acid sequences.

ACKNOWLEDGMENT

We thank Professor C. K. Chang for the initial gift of 2-OMH.

REFERENCES

Adar, F. (1978) in *The Porphyrins* (Dolphin, D., Ed.) Vol. 7, pp 167−210, Academic, New York.
Ahmad, M. B., & Kincaid, J. R. (1983) *Biochem. J. 215*, 117−122.
Andersson, L. A., Loehr, T. M., Wu, W., Chang, C. K., & Timkvich, R. (1980) *FEBS Lett. 267*, 285−288.
Atamian, M., & Bocian, D. F. (1987) *Biochemistry 26*, 8319−8326.
Babcock, G. T. (1988) in *Biological Applications of Raman Spectroscopy* (Spiro, T. G., Ed.) Vol. 3, pp 293−346, Wiley, New York.
Betz, S. F., Raleigh, D. P., & DeGrado, W. F. (1993) *Curr. Opin. Struct. Biol. 3*, 601-610.
Chang, C. K., & Wang, C.-B. (1982) in *Electron Transport and Oxygen Utilization* (Ho, C., Ed.) pp 237−243, Elsevier, New York.
Chang, C. K., & Wu, W. (1986) *J. Org. Chem. 51*, 2134−2137.
Ching, Y., Ondrias, M. R., Rousseau, D. L., Muhoberac, B. B., & Wharton, D. C. (1982) *FEBS Lett. 138*, 239−244.
Choi, S., Spiro, T. G., Langry, K. C., Smith, K. M., Budd, D. L., & La Mar, G. N. (1982) *J. Am. Chem. Soc. 104*, 4345−4351.
Choma, C. T., Lear, J. D., Nelson, M. J., Dutton, P. L., Robertson, D. E., & DeGrado, W. F. (1994) *J. Am. Chem. Soc. 11*6, 856−865.
Collman, J. P. (1977) *Acc. Chem. Res. 10*, 265−273.
Crofts, A. R., Robinson, H., Andrew, K., van Doren, S., & Berry, E. (1987) in *Cytochrome Systems: Molecular Biology and Bioenergetics* (Papa, S., Chance, B., & Ernster, L., Eds.) pp 617−624, Plenum, New York.
DeGrado, W. F., Wasserman, Z. R., & Lear, J. D. (1989) *Science 243*, 622−628.
DeGrado, W. F., Raleigh, D. P., & Handel, T. (1991) *Curr. Opin. Struct. Biol. 1*, 984-993.
Docherty, J. C., & Brown, S. B. (1982) *Biochem. J. 207*, 583−587.
Dolphin, D., Ed. (1979) *The Porphyrins*, Vol. 7, Academic, New York.
Ghadiri, M. R., & Ferhholtz, A. K. (1990) *J. Am. Chem. Soc. 112*, 9633−9635.
Gadiri, M. R., & Case, M. A. (1993) *Angew. Chem., Int. Ed. Engl. 32*, 1594−1597.
Ghadiri, M. R., Soares, C., & Choi, C. (1992a) *J. Am. Chem. Soc. 114*, 825−831.

Ghadiri, M. R., Soares, C., & Choi, C. (1992b) *J. Am. Chem. Soc. 114*, 4000−4002.
Gersonde, K., Yu, N.-T., Lin, S. H., Smith, K. M., & Parrish, D. W. (1989) *Biochemistry 28*, 3960−3966.
Gunner, M. R., & Honig, B. (1991) *Proc. Natl. Acad. Sci. U.S.A. 88*, 9151−9155.
Handel, T. M., Williams, S. A., & DeGrado, W. F. (1993) *Science 261*, 879−885.
Hecht, M. H., Richardson, J. S., Richarson, D. C., & Ogden, R. C. (1990) *Science 249*, 884−891.
Hildebrandt, P., Garda, H., Stier, A., Bachmanova, G. I., Kanaeva, I. P., & Archakov, A. I. (1989) *Eur. J. Biochem. 186*, 383−388.
Hildebrandt, P., Heibel, G., Anzenbacher, P., Lange, R., Krüger, V., & Stier, A. (1994) *Biochemistry 33*, 12920−12929.
Howell, N., & Gilbert, K. (1987) in *Cytochrome Systems: Molecular Biology and Bioenergetics* (Papa, S., Chance, B., & Ernster, L., Eds.) pp 617−624, Plenum, New York.
Ibers, J. A. & Jameson, G. B. (1994) in *Bioinorganic Chemistry* (Bertini, I., Gray, H. B., Lippard, S. J., & Valentine, J. S., Eds.) pp 167−252, University Science Books, Mill Valley, CA.
Jue, T., Krishnamoorthi, R., & La Mar, G. N. (1983) *J. Am. Chem. Soc. 105*, 5702−5704.
Kalsbeck, W. A., Ghosh, A., Pandey, R., Smith, K. M., & Bocian, D. F. (1995) *J. Am. Chem. Soc. 117*, 10959−10968.
Kitagawa, T., & Ozaki, Y. (1987) *Struct. Bonding 64*, 71−114.
Krawczyk, S. (1989) *Biochim. Biophys. Acta 976*, 140−149.
La Mar, G. N., Budd, D. L., Viscio, D. B., Smith, K. M., & Langry, K. C. (1978) *Proc. Natl. Acad. Sci. U.S.A. 75*, 5755−5759.
La Mar, G. N., Davis, N. L., Parish, D. W., & Smith, K. M. (1983) *J. Mol. Biol. 168*, 887−896.
La Mar, G. N., Toi, H., & Krishnamoorthi, R. (1984) *J. Am. Chem. Soc. 106*, 6395−6401.
Lecomte, J. T. J., Johnson, R. D., & La Mar, G. N. (1985) *Biochim. Biophys. Acta 829*, 268−274.
Lieberman, M., & Sasaki, T. (1991) *J. Am. Chem. Soc. 113*, 1470−1471.
Lutz, M., & Robert, B. (1988) in *Biological Applications of Raman Spectroscopy* (Spiro, T. G., Ed.) Vol. 3, pp 347−412, Wiley, New York.
Makinen, M., & Churg, A. K. (1983) in *Iron Porphyrins* (Lever, A. P. B., & Gray, H. B., Eds.) Vol. 1, pp 141−236, Addison-Wesley, Reading, MA.
Miki, K., Ii, Y., Owatari, A., Kai, Y., Tanaka, N., Kasai, N., Hata, Y., Kakudo, M., Katsube, Y., Kawabe, K., Yoshida, Z., Ogoshi, H., & Takano, T. (1981) *Acta Crystallogr. A37 (Suppl.)*, C-27.
Mylrajan, M., Anderrson, L. A., Loehr, T. M., Wu, W., & Chang, C. K. (1991) *J. Am. Chem. Soc. 113*, 5000−5005.
Palaniappan, V., & Bocian, D. F. (1995) *J. Am. Chem. Soc. 117*, 3647−3648.
Palmer, G. (1983) in *Iron Porphyrins* (Lever, A. P. B., & Gray, H. B., Eds.) Vol. 2, pp 43−88, Addison-Wesley, Reading, MA.
Procyk, A. D., & Bocian, D. F. (1992) *Annu. Rev. Phys. Chem. 43*, 465−496.
Rabanal, F., DeGrado, W. F., & Dutton, P. L. (1996) *J. Am. Chem. Soc. 118*, 473−474.
Regan, L., & Clarke, N. L. (1990) *Biochemistry 29*, 10878−10883.
Robertson, D. E., Farid, R. S., Moser, C. C., Urbauer, J. L., Mulholland, S. E., Pidikiti, R., Lear, J. D., Wand, A. J., DeGrado, W. F., & Dutton, P. L. (1994) *Nature 368*, 425−432.
Sarast, M. (1984) *FEBS Lett. 166*, 367−372.
Sasaki, T.,& Kaiser, E. T. (1989) *J. Am. Chem. Soc. 111*, 380−381.
Scheer, H., Ed. (1991) *Chlorophylls*, CRC Press, Boca Raton, FL.
Schick, G. A., & Bocian, D. F. (1987) *Biochim. Biophys. Acta 895*, 127−154.
Smith, K. M., Fujinari, E. M., Langry, K. C., Parish, D. W., & Tabba, H. D. (1983) *J. Am. Chem. Soc. 105*, 6638−6646.
Smith, K. M., Parish, D. W., & Inouye, W. S. (1986) *J. Org. Chem. 51*, 666−671.
Smulevich, G., English, A. M., Mantini, A. R., & Marzocchi, M. P. (1991) *Biochemistry 30*, 772−779.
Spiro, T. G. (1983) in *Iron Porphyrins* (Lever, A. P. B., & Gray, H. B., Eds.) Vol. 2, pp 89−160, Addison-Wesley, Reading, MA.
Spiro, T. G., Ed. (1988) *Biological Applications of Raman Spectroscopy*, Vol. 3, Wiley, New York.
Terner, J., & Reed, D. E. (1984) *Biochim. Biophys. Acta 789*, 80−86.
Ungashe, S. B., & Groves, J. T. (1994) in *Models in Inorganic Chemistry* (Eichhorn, G. L., Marzilli, L., Eds.) Vol. 9, pp 317−352, PRT Prentice Hall, Englewood Cliffs, NJ.
Wasielewski, M. (1992) *Chem. Rev. 92*, 435−461.
Yun, C.-H., Crofts, A. R., & Gennis, R. B. (1991) *Biochemistry 30*, 6747−6754.

BI952662K